



Effects of the oxidants H_2O and CrF_3 on the corrosion of pure metals in molten (Li,Na,K)F

Yan Li Wang, Qian Wang, Hui Jun Liu*, Chao Liu Zeng

Laboratory for Corrosion and Protection, Institute of Metal Research, Chinese Academy of Sciences, Shenyang 110016, PR China

ARTICLE INFO

Article history:

Received 15 September 2015

Received in revised form

27 November 2015

Accepted 28 November 2015

Available online 2 December 2015

Keywords:

Ni

Fe

Cr

Molten (Li,Na,K)F

Corrosion

ABSTRACT

The effects of two oxidizing species, H_2O and CrF_3 , on the corrosion of pure metals Ni, Fe and Cr in molten (Li,Na,K)F at 700 °C were investigated by potentiodynamic polarization and electrochemical impedance spectroscopy. The results indicated that Ni, Fe and Cr were all in active dissolution state at the corrosion potential and the corrosion current densities were significantly increased when 2% H_2O was introduced. However, the addition of CrF_3 only accelerated the dissolution of Cr and Fe. Based on the impedance results, the diffusion coefficient of Cr^{3+} in the melt has been calculated to be $6.25 \times 10^{-4} \text{ cm}^2 \text{ s}^{-1}$.

© 2015 Elsevier Ltd. All rights reserved.

1. Introduction

Molten fluoride salts appear to be excellent candidates as primary reactor coolant and liquid fuel in a Molten Salt Reactor (MSR) due to their advantages of good thermal conductivity, large specific heat, low viscosity, low vapor pressure at operating temperature, low melting point, high boiling point, relatively good chemical inertness, etc. [1]. However, the corrosion of structural materials in molten fluoride salts at high temperature has always been a difficult issue for the development of MSR [2]. In conventional high temperature environments, materials derive their resistance to corrosion from the formation of a dense protective oxide film such as Cr_2O_3 , Al_2O_3 or SiO_2 on their surface [3–5]. However, most metal oxides are chemically unstable in molten fluorides, and generally they are converted to the corresponding metal fluorides. The corrosion occurs mainly through the dissolution of alloying elements into the melts. Metals with less negative Gibbs free energies of fluoride formation are less prone to corrosion. According to literature [6], the Gibbs free energy of molten salts at 850 °C such as LiF, NaF and KF are more negative than that of the most metal fluorides formed during metal dissolution. For the metals typically used in contact with molten fluoride salts, the Gibbs free energy increases in the following order: Ni, Co, Fe, Cr and Al, which means

that Ni is the most noble in this list. In addition, more noble metals with a low content of Cr are suitable for the structural materials for MSR, among which Hastelloy-N (Ni-16%Mo-7%Cr-5%Fe, weight percent) developed by Oak Ridge National Laboratory has been successfully used as the container material of an experimental molten salt reactor [7,8].

The main driving forces for the corrosion in molten fluorides are generally involved with the impurities in fluorides, temperature gradients and activity gradients. The oxidizing impurities in fluoride salts such as H_2O and metal oxides have been considered as the main oxidizing driving forces [9]. As a common impurity, H_2O , is extremely hard to be removed completely. It may react with molten fluorides to generate HF, which then attacks metals to form metal fluorides. The increase in the content of impurities may make the melts more aggressive, and thus enhance the corrosion rate. In a study of the effect of moisture on the corrosion of Ni-based alloys in molten (Li,Na,K)F, Ouyang et al. observed that higher moisture content would aggravate intergranular corrosion and pitting [10]. Kondo et al. also reported that the corrosion of JLF-1(Fe-9Cr-2W-0.1C) in the purified (Li,Na,K)F was much less than that in the non-purified (Li,Na,K)F [11].

In addition to the impurity H_2O , some metal fluoride contaminants in the melt, such as NiF_2 or FeF_2 , can oxidize Cr due to their more positive free energy of fluoride formation. Of chromium, iron and nickel as the most common metals in alloys, Cr is more susceptible to attack in molten fluorides. Cr is dissolved into the melt to form Cr^{2+}/Cr^{3+} , with Cr^{3+} as the primary valence state in (Li,Na,K)F [12].

* Corresponding author. Fax: +86 24 23904551.

E-mail addresses: liuhj@imr.ac.cn, hjiu2003@aliyun.com (H.J. Liu).

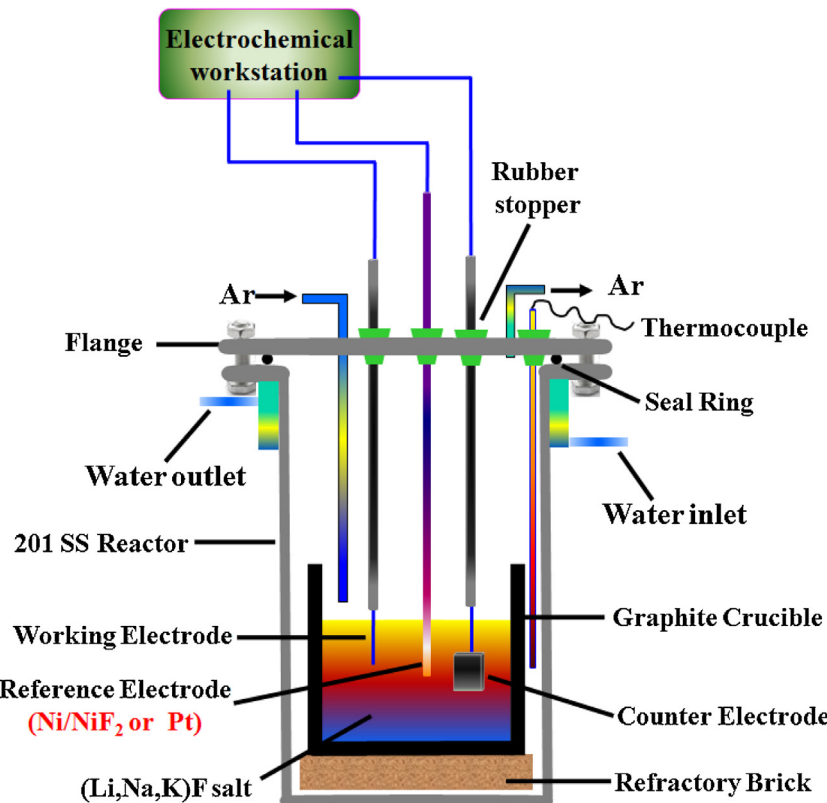


Fig. 1. A schematic diagram of experimental setup.

It should be noted that if substantial concentrations of multivalent transition metal ions (e.g., Cr²⁺/Cr³⁺, Fe²⁺/Fe³⁺, etc.) are present in the melt, the corrosion reaction could involve these species. CrF₃ and FeF₃ have slightly more positive Gibbs free energies than their corresponding CrF₂ and FeF₂ [6], thus cations of greater valence of polyvalent transition metals, such as Fe³⁺ and Cr³⁺, are also potential oxidants that can cause the oxidation of their own base metal and other metals [9]. In (Li,Na,K)F, CrF₃ contaminant in solution can promote the corrosion of the zero-state Cr metal by the following inverse disproportionation reaction [9]:



Olson et al. [6] observed that the Cr³⁺/Cr²⁺ accelerated the corrosion process of the Incoloy-800H alloy in electric contact with a graphite crucible in molten (Li,Na,K)F. It was suggested that the cation Cr²⁺ formed by the oxidation of Cr⁰ and disproportionately evolves to higher valent cation Cr³⁺ and chromium carbides at the graphite surface. The inverse disproportionation product Cr³⁺ can diffuse back to the alloy surface and be reduced to Cr²⁺. It is clear that Cr³⁺ can act as an oxidizer to accelerate the oxidation of the alloy. In the above corrosion system, galvanic corrosion actually occurs because the graphite crucible and the alloy Incoloy-800H with different electromotive potentials were in electric contact in the melt. In fact, chromium ions dissolved from the alloy (anode) could diffuse toward the graphite crucible (cathode) and be reduced

directly to form chromium carbides. In a study of galvanic corrosion of pure Ni, Fe and Cr in molten fluorides, small amounts of anodic metals-containing products were observed to form on the surface of cathodic metals after galvanic corrosion measurements, probably due to the fact that the dissolved Cr or Fe ions can diffuse toward the cathode to be reduced partially [13]. Moreover, it is still unclear if the above mechanism can be used to describe the corrosion of alloy without electric contact with the graphite crucible in the melt. Unfortunately, there are limited reports on the effect of Cr³⁺ on the corrosion of alloys in molten fluorides, and thus a detailed affecting mechanism of Cr³⁺ is still to be investigated extensively.

In the present study, due to the fact that the mean operating temperature and the core outlet temperature of molten salt in MSR are 700 °C, the open circuit potential, potentiodynamic polarization and electrochemical impedance spectroscopy are employed to examine the effect of oxidants H₂O and CrF₃ on the corrosion of three pure metals Ni, Fe and Cr in molten (Li,Na,K)F at 700 °C.

2. Experimental procedures

The materials used in the present study are Ni (99.96 wt.% purity), Fe (99.87 wt.% purity), and Cr (99.19 wt.% purity). The bulk metals were cut into samples with a size of 5 mm × 30 mm × 2 mm by an electric spark cutter, followed by grinding down to 1000 grit

Table 1

Electrochemical parameters obtained by Tafel linear fitting of IR-corrected polarization curves for Ni, Fe and Cr in molten (Li,Na,K)F at 700 °C.

Metals	b_a (mV dec ⁻¹) Ar	b_a (mV dec ⁻¹) Ar-2% H ₂ O	b_c (mV dec ⁻¹) Ar	b_c (mV dec ⁻¹) Ar-2% H ₂ O	E_{corr} (mV vs. Ni/NiF ₂) Ar	E_{corr} (mV vs. Ni/NiF ₂) Ar-2% H ₂ O	I_{corr} (mA cm ⁻²) Ar	I_{corr} (mA cm ⁻²) Ar-2% H ₂ O
Ni	161.6	143.5	-141.8	-125.9	-77	-50	0.0193	0.150
Fe	138.5	53.5	-332.0	-133.1	-338	-300	0.261	1.425
Cr	173.3	62.2	-140.5	-273.9	-507	-450	0.494	3.715

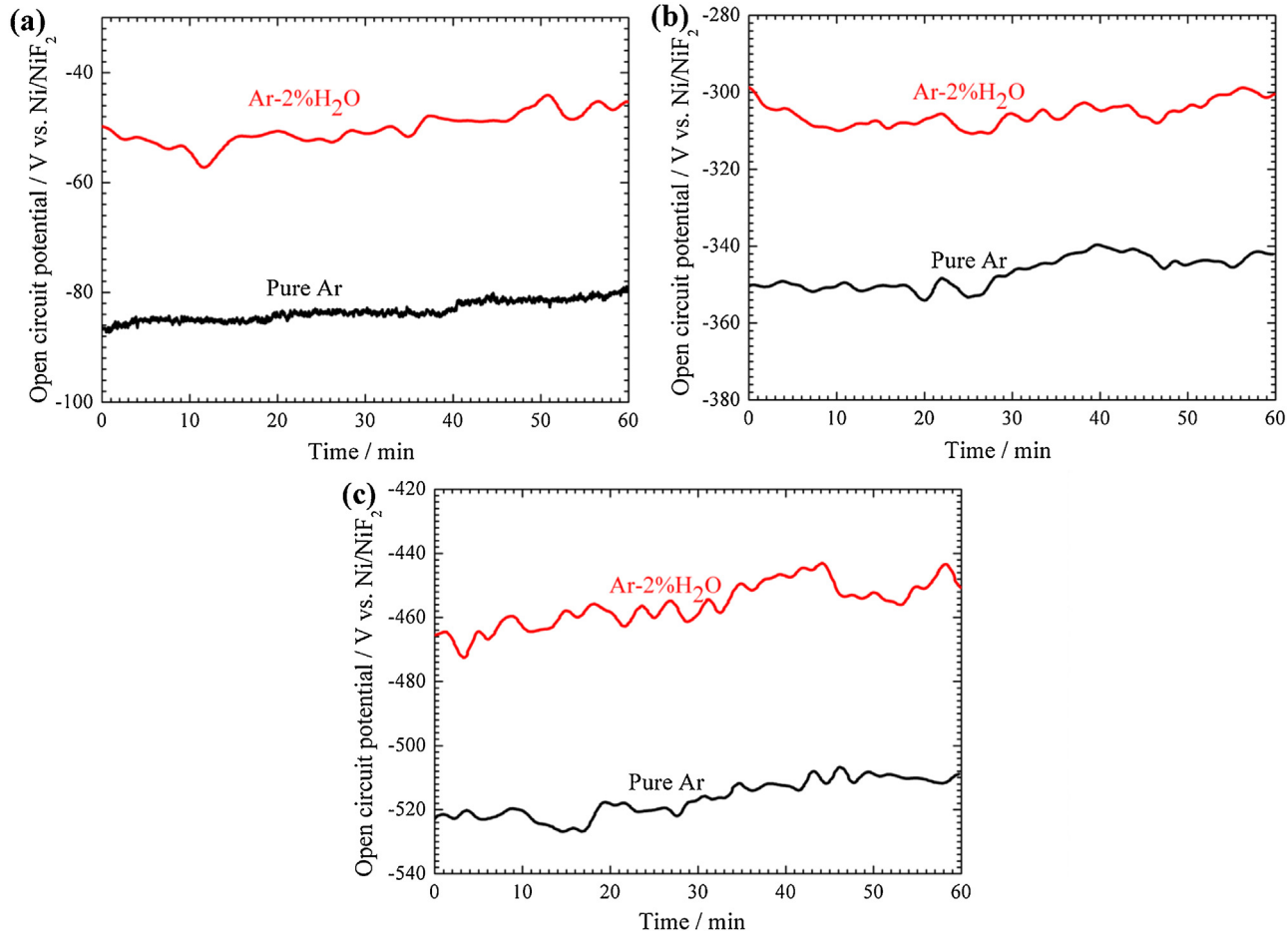


Fig. 2. The open circuit potential for Ni (a), Fe (b), and Cr (c) in molten (Li,Na,K)F at 700 °C under Ar and Ar-2% H_2O environments.

SiC paper, rinsing with distilled water and then drying with an electric hair drier. A Fe–Cr wire was spot welded to one end of the specimens for electrical connection. The welded spot and the partial sample were sealed in an alumina tube with high-temperature cement, with a length of 15 mm exposed, followed by standing for 24 h at room temperature and curing at 300 °C for 2 h. The exposed surfaces of samples were ground again with 1000 grit SiC paper, rinsed with acetone and then dried with an electric hair drier before tests.

All experiments were conducted in a closed stainless steel chamber under a protection of circulating high-purity argon, as shown in Fig. 1. A eutectic mixture of 46.5%LiF-11.5%NaF-42%KF (mol%) was used for the corrosion test. After drying the LiF, NaF and KF (supplied by Sinopharm Chemical Reagent Co., Ltd., China), respectively, at 200 °C in vacuum, a 178.6 g mixture of (Li,Na,K)F was put into a graphite crucible. The mixed salts were further dried at 200 °C in the experimental apparatus under vacuum for at least 48 h, and then the furnace was heated to the experimental temperature of 700 °C under the protection of flowing high-purity argon. To investigate the effect of water vapor on the corrosion behavior of the metals in molten (Li,Na,K)F, the Ar was allowed to pass through a closed isothermal water box to produce wet Ar before flowing into the reaction chamber. The temperature of the water box was kept at 18 °C corresponding to 2% water vapor. Additionally, CrF₃ with concentrations of 0.09 and 0.18 M was also added to the (Li,Na,K)F eutectic salt, in an attempt to clarify the effect of high valence Cr³⁺ on the corrosion of pure metals in molten (Li,Na,K)F.

Electrochemical measurements including open circuit potential, potentiodynamic polarization and electrochemical impedance were conducted in the melt at 700 °C with a Princeton Applied Research PARSTAT 2273 potentiostat/Galvanostat system. All electrochemical tests were started after the working electrodes are immersed in molten (Li,Na,K)F for at least 30 min to reach a steady state. Potentiodynamic polarization was undertaken at a scan rate of 20 mV min⁻¹, using a conventional three-electrode system with a Ni/NiF₂ electrode or a Pt electrode as the reference electrode (RE) and a high-density graphite plate (supplied by Sinosteel Shang-hai Advanced Graphite Materials Company, China) with the dimension of 30 mm × 15 mm × 3 mm as the counter electrode. The Ni/NiF₂ electrode is self-made by placing a Ni wire with a diameter of 0.5 mm in a close-ended Boron nitride tube (dia. 12 mm) which was filled with 10 g (Li,Na,K)F-10 wt.% NiF₂. The graphite counter electrode exhibits high chemical stability in molten (Li,Na,K)F. During potentiodynamic polarization tests, the reduction reactions occurring on the graphite electrode as a cathode mainly include the reduction of HF, Cr³⁺, Fe³⁺, etc., and the oxidation reactions as an anode mainly include the oxidation of some lower valent metal ions such as Fe²⁺, Cr²⁺, etc. These reduction or oxidation reaction products would not affect the composition of the working electrolyte. Although molten (Li,Na,K)F has good electrical conductivity [14], polarization data would be inspected for IR drop. Electrochemical impedance measurements using a two-electrode system (two working electrodes) were carried out at open circuit potential between 0.01 Hz and 100 kHz, with amplitude of 10 mV.

The corroded samples covered with the remaining salts were mounted in epoxy resin and then their metallurgical sections were prepared by using kerosene as coolant for grinding and polishing, with an attempt to examine the metal/salt interface. The cross-sectional morphology of the samples was characterized by scanning electron microscope (SEM) coupled with an energy dispersive X-ray spectrometer (EDX).

3. Results

3.1. Effect of H_2O on the corrosion in molten (Li,Na,K)F

Fig. 2 gives the open circuit potential (OCP) for Ni, Fe and Cr in molten (Li,Na,K)F at 700 °C under Ar and Ar-2% H_2O , respectively. The results reveal that the OCP for Ni maintains at -80 and -50 mV vs. Ni/NiF_2 with some fluctuation under Ar and Ar-2% H_2O , respectively. The OCP for Fe also shows obvious fluctuation around -330 and -300 mV vs. Ni/NiF_2 under Ar and Ar-2% H_2O , respectively. Cr shows the most negative potential at -510 and -450 mV vs. Ni/NiF_2 under Ar and Ar-2% H_2O , respectively. **Fig. 3(a), (c) and (e)** shows the raw data potentiodynamic polarization curves of Ni, Fe and Cr in molten (Li,Na,K)F at 700 °C under Ar and Ar-2% H_2O environments, respectively. Based on the experimental impedance results for the corrosion of Ni in molten (Li,Na,K)F presented below, an average ohmic resistance of around $2.57\ \Omega\ cm^2$, which was determined by modeling the impedance data at the high-frequency limit of the impedance, for the working electrolyte was obtained to correct the polarization curves, as shown in **Fig. 3(b), (d) and (f)**. It is shown that three metals are all in active state at the corrosion potential under both atmospheres. The corrosion potential for Ni, Fe and Cr in Ar-2% H_2O is more positive than that in Ar, suggesting that the impurity H_2O changes the redox state of the melt, which has also been reported by Keiser et al. [15]. Moreover, both the anodic and cathodic reaction current densities have been increased significantly by 2% H_2O . The corrosion potentials and corrosion current densities are obtained from the IR-corrected polarization curves via Tafel method, as shown in **Fig. 3(d)**. The values are listed in **Table 1**. The corrosion current densities for Ni, Fe and Cr in Ar-2% H_2O are 0.150, 1.425, and $3.715\ mA\ cm^{-2}$, compared to 0.0193, 0.261, and $0.494\ mA\ cm^{-2}$ in Ar, respectively. This indicates that the presence of 2% H_2O significantly accelerates the corrosion of the three metals.

3.2. Effect of CrF_3 on the corrosion in molten (Li,Na,K)F

Fig. 4 presents the open circuit potential for Ni, Fe, and Cr in molten (Li,Na,K)F- CrF_3 . The potential for Ni, Fe and Cr shifts positively with the addition of CrF_3 . When added 0, 0.09 and 0.18 M CrF_3 in molten (Li,Na,K)F, the OCP for Ni is about -95, -65 and -45 mV vs. Pt, respectively. However, the OCP for Fe presents obvious fluctuation around -385, -325, -310 mV vs. Pt, respectively. The OCP for Cr is around at -550, -480, -435 mV vs. Pt, with little fluctuation, respectively. **Fig. 5(a), (c) and (e)** gives the raw data potentiodynamic polarization curves of Ni, Fe, and Cr in molten (Li,Na,K)F- CrF_3 under Ar with different amounts of CrF_3 additive and the corresponding IR-corrected polarization curves are shown in **Fig. 5(b), (d) and (f)**. It is shown clearly that CrF_3 significantly enhances the cathodic reaction. Unlike the cathodic reaction, the effect of CrF_3 on the anodic reaction is different among three metals. The anodic reaction of pure Ni changes little, as shown in **Fig. 5(b)**, when CrF_3 is added, while that of Fe and Cr is enhanced.

Based on the IR-corrected polarization curves, Tafel extrapolation method, as shown in **Fig. 3 (d)**, was used to calculate the corrosion current density, and the results are shown in **Table 2**. It is shown that the I_{corr} for Cr increases by more than three times and Fe by more than one times after adding CrF_3 , while this effect

Table 2
Electrochemical parameters obtained by Tafel linear fitting of IR-corrected polarization curves for Ni, Fe and Cr in molten (Li,Na,K)F at 700 °C with and without CrF_3 , respectively.

Metals	$b_a\ (mV\ dec^{-1})$			$b_c\ (mV\ dec^{-1})$			$E_{corr}\ (mV\ vs.\ Pt)$			$I_{corr}\ (mA\ cm^{-2})$		
	0 M CrF_3	0.09 M CrF_3	0.18 M CrF_3	0 M CrF_3	0.09 M CrF_3	0.18 M CrF_3	0 M CrF_3	0.09 M CrF_3	0.18 M CrF_3	0 M CrF_3	0.09 M CrF_3	0.18 M CrF_3
Ni	80.5	72.5	66.7	-65.1	-45.4	-45.1	-92	-68	-45	0.0432	0.0459	0.0561
Fe	388.5	76.3	61.3	-196.9	-133.8	-142.5	-380	-324	-310	0.271	0.631	0.851
Cr	88.4	205.7	84.2	-140.8	-197.5	-148.4	-550	-484	-431	0.531	2.245	2.83

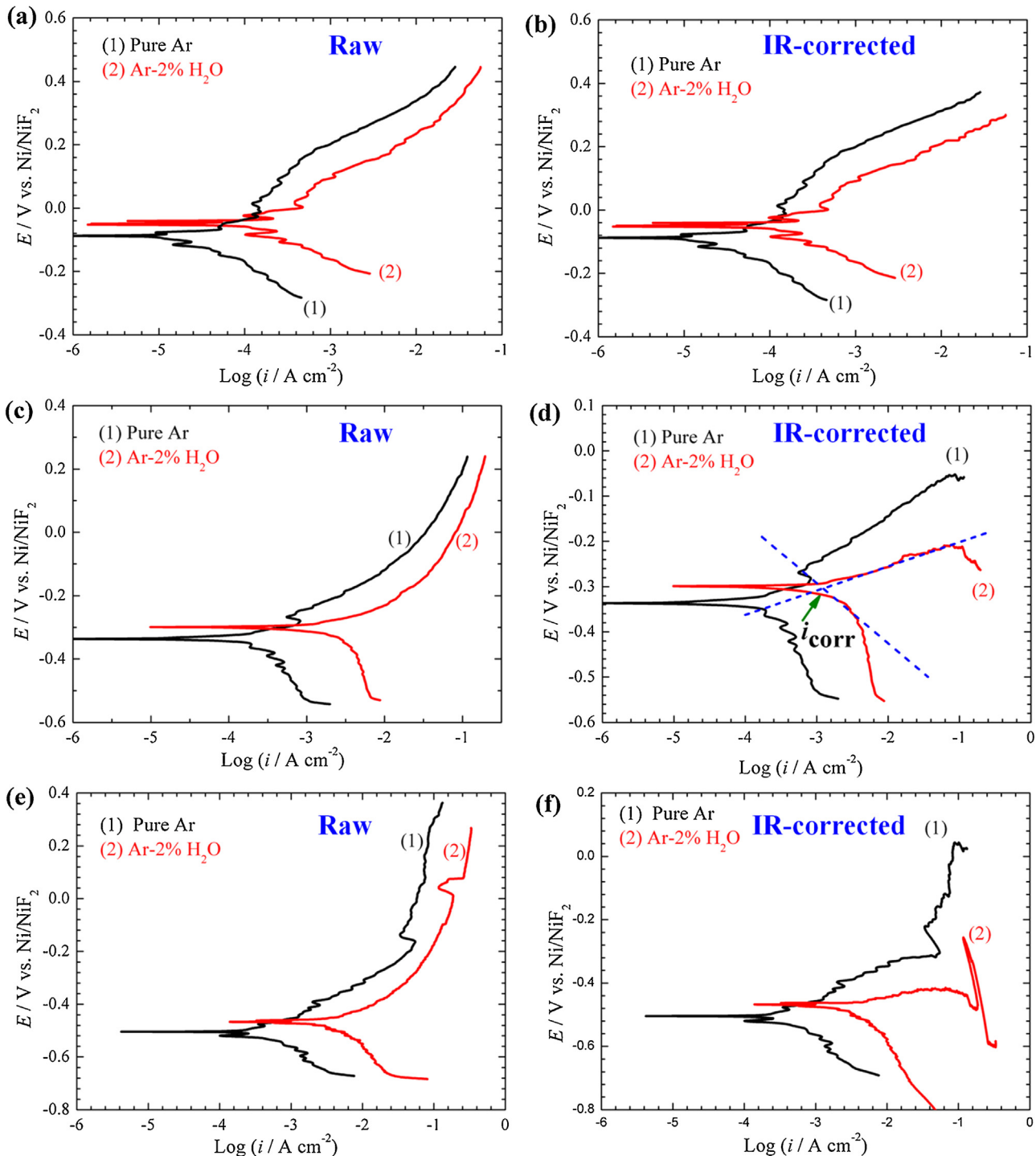


Fig. 3. Raw data polarization curves (a, c, e) together with the corresponding IR-corrected polarization curves (b, d, f) of Ni (a, b), Fe (c, d), and Cr (e, f) at 700 °C in molten (Li,Na,K)F under Ar and Ar-2% H_2O environments.

is small on the i_{corr} for Ni. The above results suggest that CrF_3 , as an oxidizer, can significantly accelerate the corrosion of Cr and Fe, especially for Cr.

Fig. 6 shows the typical Nyquist and Bode plots of Ni after corrosion in molten (Li,Na,K)F- CrF_3 at 700 °C under Ar for various intervals of time. The results show that the Nyquist plots are all similar and tend to a semicircle for the experimental duration of 50 h, pointing out to a capacitive component associated to the interface Ni/(Li,Na,K)F- CrF_3 .

Unlike Ni, the addition of CrF_3 to (Li,Na,K)F gives rise to the change of impedance features for the corrosion of Fe, as shown in Fig. 7. In the absence of CrF_3 , the Nyquist plots in molten (Li,Na,K)F tend to be a capacitive loop corroborated by the existence of a maximum point in the bode phase plot [16], however, the impedance values are smaller than that for nickel. When CrF_3 is added to (Li,Na,K)F, however, the Nyquist plots consist of two capacitive loops, i.e., a very small depressed semicircle at high frequency, as shown in the insert of Fig. 7(c) and (e), and a large depressed semicircle at low frequency. The impedance responses at high frequency

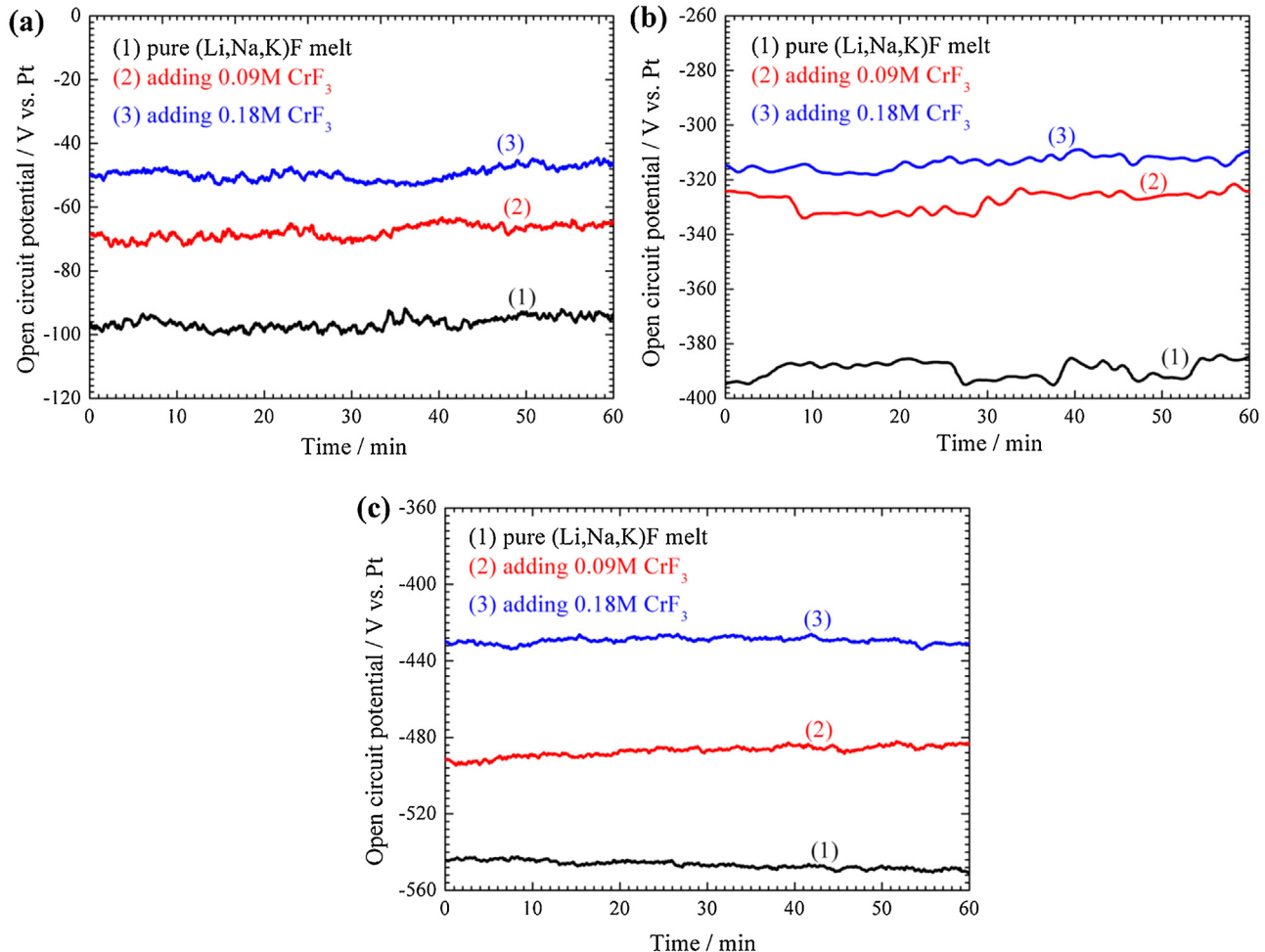


Fig. 4. The open circuit potential for Ni (a), Fe (b), and Cr (c) in molten (Li,Na,K)F with and without CrF_3 at 700°C under Ar environment.

Table 3

Fitting results of the impedance spectra for Ni in molten (Li,Na,K)F at 700°C with and without CrF_3 , respectively.

Time(h)	Molten (Li,Na,K)F		Adding 0.09 M CrF_3		Adding 0.18 M CrF_3	
	$R_s(\Omega \text{ cm}^2)$	$R_t(\Omega \text{ cm}^2)$	$R_s(\Omega \text{ cm}^2)$	$R_t(\Omega \text{ cm}^2)$	$R_s(\Omega \text{ cm}^2)$	$R_t(\Omega \text{ cm}^2)$
1	2.61	228.5	2.61	547.2	—	—
2	—	—	—	—	2.75	443.7
4	2.44	392.7	2.66	528.6	—	—
5	—	—	—	—	2.69	417.1
12	2.45	559.5	2.62	497.6	2.26	588.5
14	2.47	612.1	—	—	—	—
16	—	—	2.71	416.8	—	—
18	—	—	—	—	2.68	443.8
24	2.57	678.2	2.71	402.8	2.70	414.9
31	2.55	387.9	2.59	326.5	—	—
36	2.65	466.6	2.67	291.2	2.67	377.8
40	—	—	—	—	2.67	352.1
41	2.73	694.9	2.67	594.7	—	—
50	2.69	363.7	2.87	361.9	2.65	318.6

are probably related to the formation of a Cr ions-containing layer, while the low-frequency responses are related to the electrochemical reaction process. The phase angle θ exhibits smaller values at middle and high frequencies, suggesting a predominantly resistive behavior. Moreover, the impedance values decrease slightly with the increase in the concentration of CrF_3 in molten (Li,Na,K)F.

Fig. 8 presents the typical Nyquist and Bode plots of Cr after corrosion in molten (Li,Na,K)F- CrF_3 at 700°C under Ar for various intervals of time. The Nyquist plots for the corrosion of Cr in

molten (Li,Na,K)F are composed of a capacitive loop, with significantly smaller impedance values than those for Ni and Fe. However, when adding CrF_3 to (Li,Na,K)F, the Nyquist plots are composed of a small capacitive loop at high frequency, shown in the insert of Fig. 8(b) and (c), and a line in the low frequency range, suggesting a diffusion-controlled reaction (Warburg impedance). All of these suggest that the corrosion of Cr can be accelerated by the additive of CrF_3 .

The impedance spectra for the corrosion of Ni in the melt, those for Fe and Cr in the absence of CrF_3 could be fitted by the equivalent circuit of Fig. 9(a), and those for Fe and Cr in the presence of CrF_3 could be fitted by the equivalent circuit of Fig. 9(b) and (c), respectively. In Fig. 9, R_s represents the molten salts resistance, C_{dl} double-layer capacitance, C_c the corrosion layer capacitance, R_t charge transfer resistance, R_c the corrosion layer resistance, and Z_w the Warburg impedance. Taking into account of the dispersion effect, a constant phase angle element (CPE) Q is used to replace the element C_{dl} and C_c in fitting procedure to reflect exponential distribution of the parameters of the electrochemical reaction related to energetic barrier at charge and mass transfer, as well as impedance behavior caused by fractal surface structure [17,18]. The impedance of CPE is expressed as

$$Z_{CPE} = \frac{1}{Y_0(jw)^n} \quad (2)$$

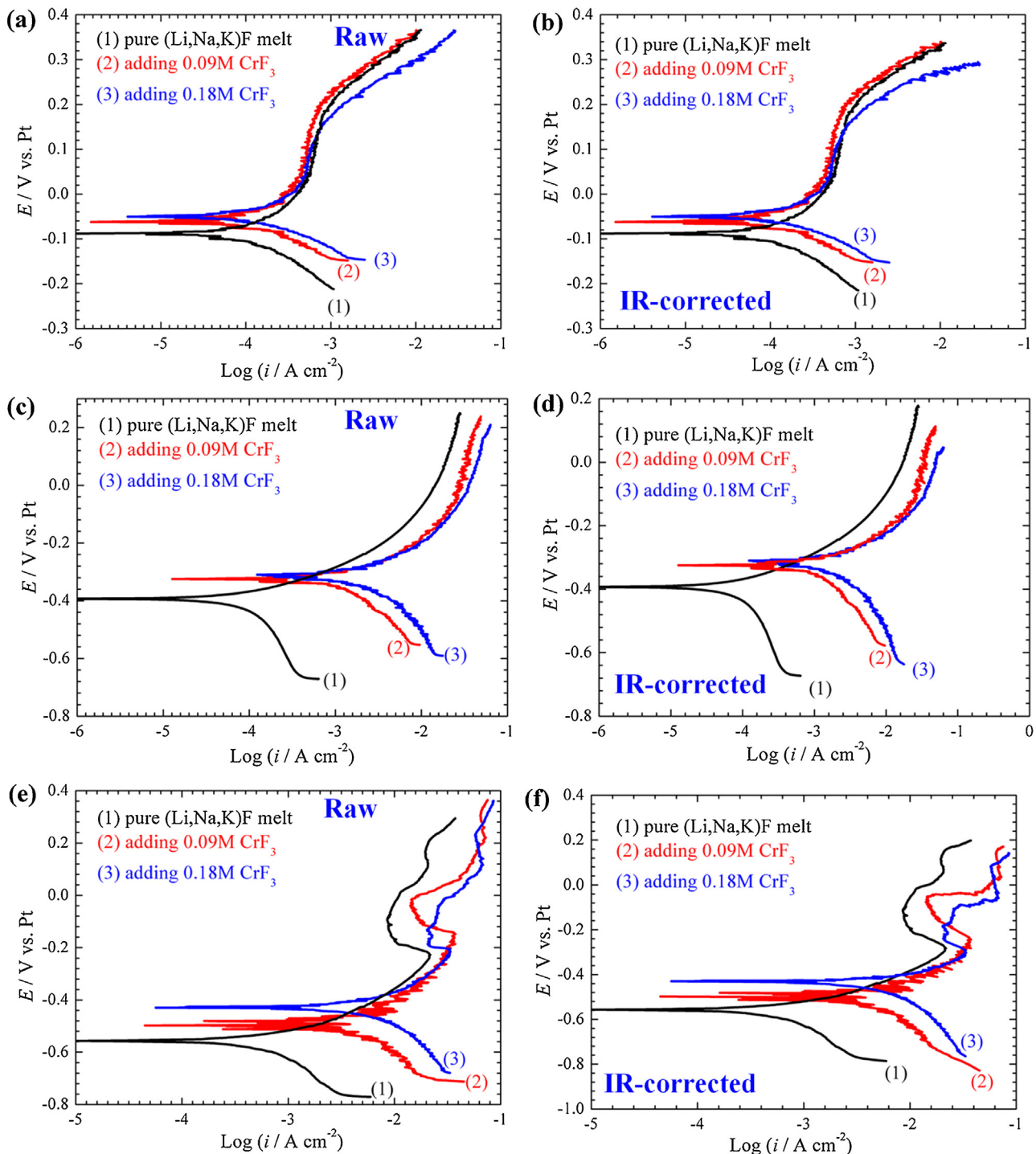


Fig. 5. Raw data polarization curves (a, c, e) together with the corresponding IR-corrected polarization curves (b, d, f) of Ni (a, b), Fe (c, d), and Cr (e, f) at 700 °C under Ar in molten (Li,Na,K)F with and without CrF₃, respectively.

Thus, the total impedance of Fig. 9(a) can be expressed by Eq. (3), that of Fig. 9(b) by Eq. (4) and that of Fig. 9(c) by Eq. (5):

$$Z = R_s + \frac{1}{Y_{dl}(jw)^{n_{dl}} + 1/R_t} \quad (3)$$

$$Z = R_s + \frac{1}{Y_c(jw)^{n_c} + 1/R_t} + \frac{1}{Y_{dl}(jw)^{n_{dl}} + 1/R_t} \quad (4)$$

$$Z = R_s + \frac{1}{Y_{dl}(jw)^{n_{dl}} + 1/R_t + Z_w} \quad (5)$$

where Y_{dl} and n_{dl} , and Y_c and n_c are constants representing the element Q_{dl} and Q_c , respectively. The Warburg impedance Z_w is expressed by Eq. (6)

$$Z_w = A_w(jw)^{-1/2} \quad (6)$$

where A_w is the coefficient of Z_w .

According to the equivalent circuits shown in Fig. 9, the impedance spectra for the corrosion of the metals have been fitted and some electrochemical parameters are listed in Tables 3–5, respectively. Figs. 6–8 clearly show that the experi-

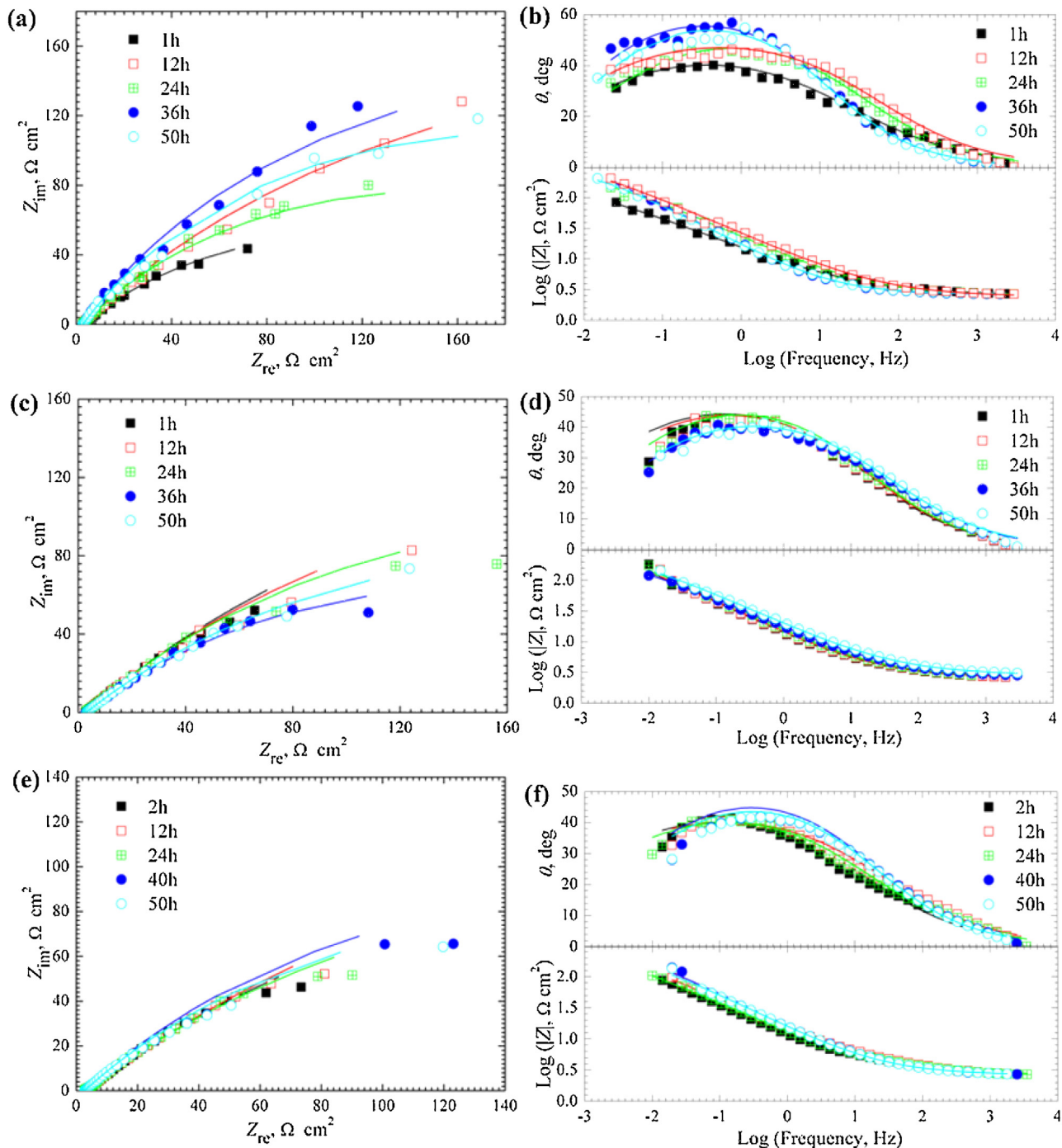


Fig. 6. Bode and Nyquist plots for the corrosion of Ni in molten (Li,Na,K)F added 0 M ((a) and (b)), 0.09 M ((c) and (d)) and 0.18 M ((e) and (f)) CrF₃ at 700 °C under Ar environment. Symbol: experimental data; line: simulation data.

mental data are accurately fitted by the equivalent circuit of the AC impedance diagram as shown in Fig. 9, which indicating that the proposed equivalent circuits are reasonable.

Table 3 indicates that the values of R_t for the corrosion of Ni in the melts are in the order of several hundreds $\Omega \text{ cm}^2$, and change little with the concentrations of CrF₃, suggesting that the corrosion of Ni is not affected by CrF₃. In addition, the values of R_s are around $2.6 \Omega \text{ cm}^2$, suggesting a good electrical conductivity of the molten salt.

Table 4 shows that the values of R_t for the corrosion of Fe in the melts are decreased with the increasing of CrF₃ concentration. In

addition, the values of R_t are significantly smaller than those for Ni compared to Table 3. Therefore, we can conclude that the corrosion of Fe could be promoted by CrF₃.

R_t for the corrosion of Cr in the melts is significantly smaller than that for both Ni and Fe, and decreases obviously with the addition of CrF₃, from the values of around $3 \Omega \text{ cm}^2$ to the values less than $1 \Omega \text{ cm}^2$, as shown in Table 5. Therefore, the dissolution of Cr could be significantly accelerated by the additive of CrF₃. These results are in a good agreement with the potentiodynamic polarization results.

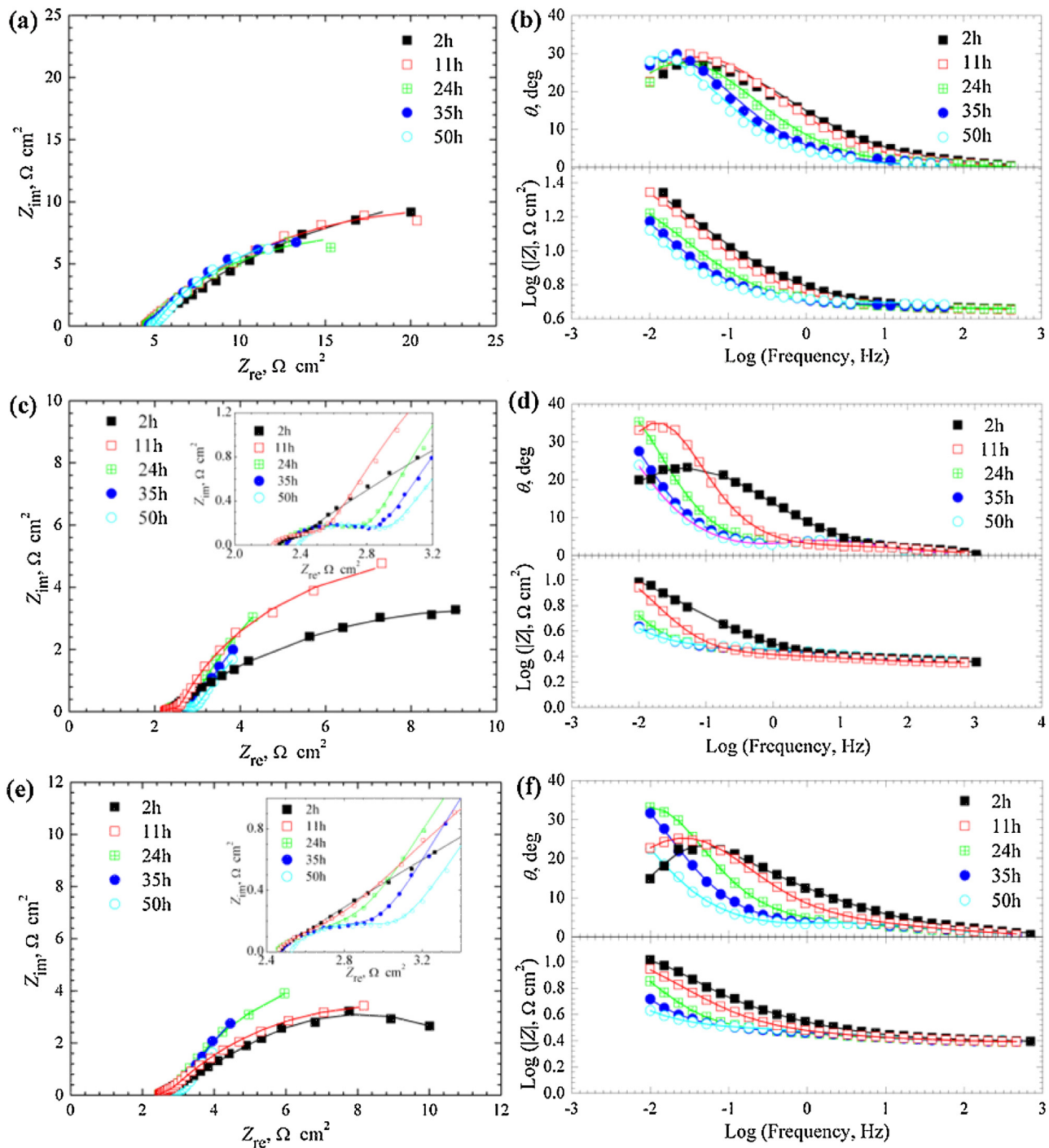


Fig. 7. Bode and Nyquist plots for the corrosion of Fe in molten (Li,Na,K)F with 0 M ((a) and (b)), 0.09 M ((c) and (d)) and 0.18 M ((e) and (f)) CrF_3 at 700 °C under Ar environment. Symbol: experimental data; line: simulation data.

3.3. Characterizations of the corroded samples

To examine the corroded melt/salt mixture interface, the cross sections of the corroded samples covered with the remaining salts were prepared for SEM observations. Fig. 10 presents the cross-sectional morphologies of Ni after immersion in the melt with and without CrF_3 at 700 °C under Ar for 50 h. The results show that Ni suffers from a slight non-uniform dissolution depicted by small surface asperities (height lower than 10 μm). This indicates that CrF_3 has a little effect on the corrosion of Ni in molten (Li,Na,K)F.

Fig. 11 shows the cross-sectional morphologies of Fe corroded in the melt at 700 °C under Ar for 50 h. The dissolution of Fe in molten (Li,Na,K)F was more non-uniform compared to Ni. However, when adding CrF_3 to the melt, the dissolution of Fe tends to be more non-uniform. Moreover, some Cr and Fe enriched fluorides are observably formed in the melt near the metal/melt surface (Fig. 11(b) and (c)). Cr also experiences non-uniform dissolution in the melt with and without CrF_3 at 700 °C under Ar, as shown in Fig. 12. Furthermore, in the local area, some Cr-rich products are also detected.

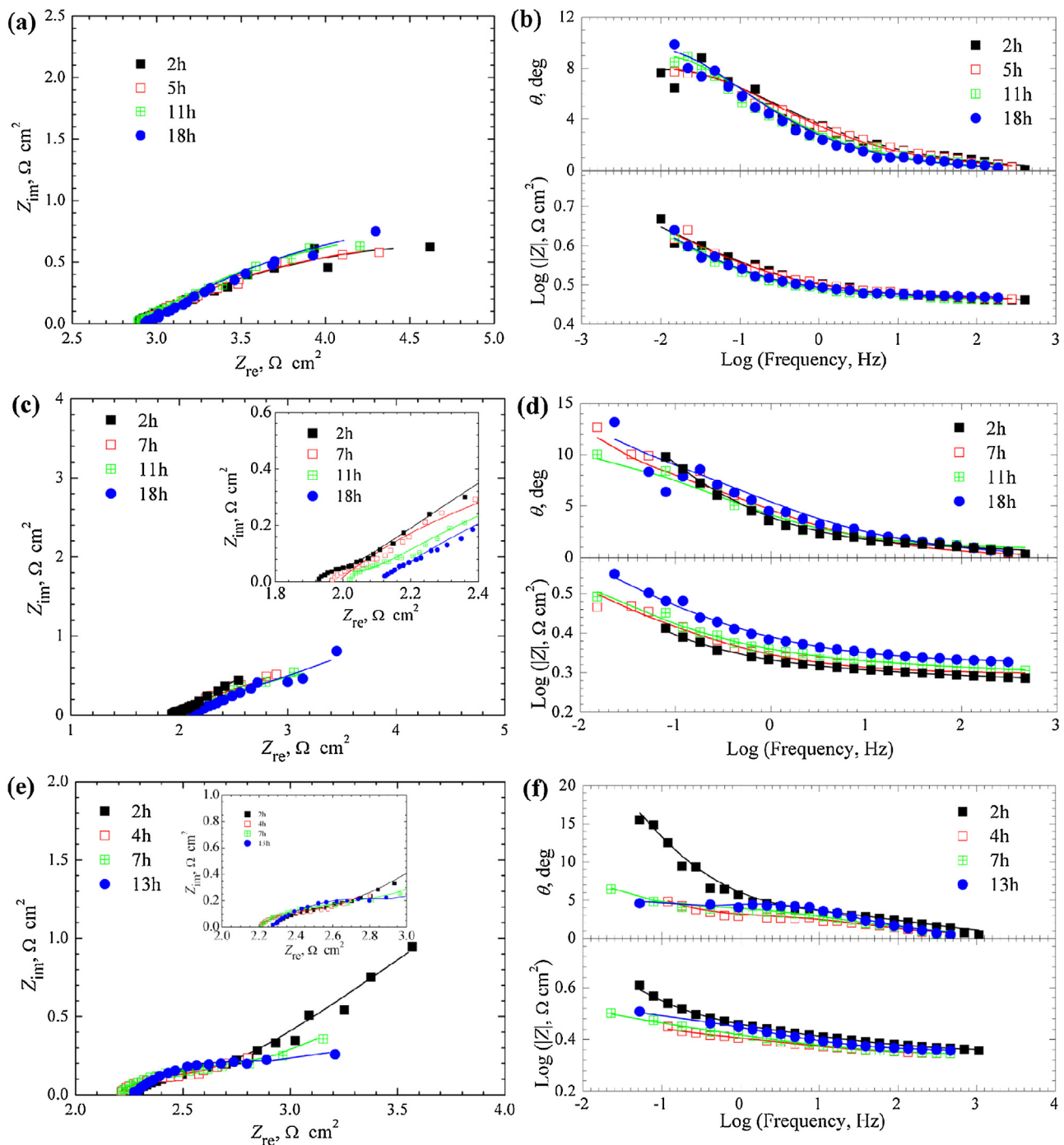


Fig. 8. Bode and Nyquist plots for the corrosion of Cr in molten (Li,Na,K)F added 0 M ((a) and (b)), 0.09 M ((c) and (d)) and 0.18 M ((e) and (f)) CrF₃ at 700 °C under Ar environment. Symbol: experimental data; line: simulation data.

4. Discussion

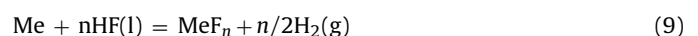
The above results show that the impurity H₂O obviously accelerates the corrosion of Ni, Fe, and Cr, while high-valence Cr ions (CrF₃) could only enhance greatly the corrosion of Cr and Fe, especially Cr, with little effect on the corrosion of Ni. It is clear that the impurity H₂O could act as an effective oxidizing species to accelerate the dissolution of some common metals such as Ni, Fe and Cr, while CrF₃ could only advance the corrosion of Cr and Fe examined in the present study.

H₂O is among the most deleterious impurities in molten fluorides from the viewpoint of corrosion and is extremely hard to be

removed completely. At high temperatures, H₂O may react with fluorides to generate gaseous HF by the following reactions:



M = Li, Na, K. The generated HF may be dissolved partially into the melt and react with metals to form soluble metal fluorides:



Me = Ni, Fe, Cr.

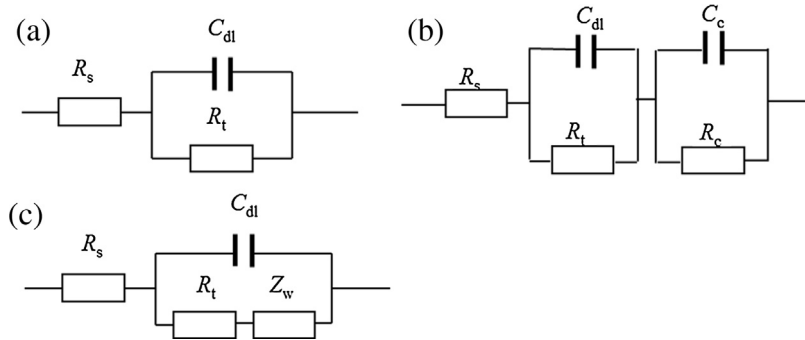


Fig. 9. Equivalent circuits representing the impedance spectra for the corrosion of Ni (a) and Fe ((a) and (b)) and Cr ((a) and (c)) in molten (Li,Na,K)F with and without CrF_3 at 700 °C under Ar environment.

Table 4

Fitting results of the impedance spectra for Fe in molten (Li,Na,K)F at 700 °C with and without CrF_3 , respectively.

Time(h)	Molten (Li,Na,K)F		Adding 0.09 M CrF_3			Adding 0.18 M CrF_3		
	$R_s(\Omega \text{ cm}^2)$	$R_t(\Omega \text{ cm}^2)$	$R_s(\Omega \text{ cm}^2)$	$R_t(\Omega \text{ cm}^2)$	$R_c(\Omega \text{ cm}^2)$	$R_s(\Omega \text{ cm}^2)$	$R_t(\Omega \text{ cm}^2)$	$R_c(\Omega \text{ cm}^2)$
2	4.55	45.39	2.27	14.74	0.04961	2.45	13.9	0.178
4	4.52	50.52	2.26	10.93	0.2438	2.47	13.2	0.132
6	–	–	–	–	–	2.46	14.1	0.220
7	4.49	39.19	2.23	12.90	0.2438	–	–	–
11	4.50	35.27	2.21	13.06	0.3736	2.45	12.1	0.333
15	–	–	–	–	–	2.45	12.9	0.328
16	–	–	2.23	15.92	0.4376	–	–	–
24	4.60	25.27	2.26	20.37	0.5568	2.43	13.0	0.620
28	–	–	–	–	–	2.42	17.5	0.662
35	4.76	26.40	2.30	26.47	0.5706	2.46	21.4	0.556
40	4.81	26.17	2.33	12.73	0.5771	–	–	–
42	–	–	–	–	–	2.48	18.0	0.596
50	4.93	25.96	2.38	21.88	0.550	2.51	35.5	0.579

Table 5

Fitting results of the impedance spectra for Cr in molten (Li,Na,K)F at 700 °C with and without CrF_3 , respectively.

Time(h)	Molten (Li,Na,K)F		Adding 0.09 M CrF_3			Adding 0.18 M CrF_3		
	$R_s(\Omega \text{ cm}^2)$	$R_t(\Omega \text{ cm}^2)$	$R_s(\Omega \text{ cm}^2)$	$R_t(\Omega \text{ cm}^2)$	$A_w(\Omega \text{ cm}^2 \text{ s}^{-0.5})$	$R_s(\Omega \text{ cm}^2)$	$R_t(\Omega \text{ cm}^2)$	$A_w(\Omega \text{ cm}^2 \text{ s}^{-0.5})$
2	2.88	3.73	1.88	0.243	0.929	2.24	0.614	1.073
3	–	–	–	–	–	2.15	0.914	0.1088
4	–	–	1.96	0.819	0.635	2.18	0.507	0.2704
5	2.90	3.50	–	–	–	–	–	–
7	–	–	1.98	1.36	0.295	2.17	0.962	0.1862
8	2.84	2.23	–	–	–	–	–	–
11	2.89	3.70	1.81	0.495	1.425	–	–	–
13	–	–	2.03	0.839	0.396	2.25	0.890	0.1669
15	2.92	2.29	–	–	–	–	–	–
18	2.94	3.93	2.11	2.40	0.386	–	–	–

The increase of the impurity H_2O could increase the redox potential of the melt and thus make the melt be more corrosive to metals. An investigation by Ignat'ev et al. has indicated that the redox potential of $\text{NaF}-\text{LiF}-\text{BeF}_2$ could be decreased from 1.78 to 1.10 V relative to a beryllium reference electrode by removing the impurities from the melt [19]. When 2% H_2O was added into the reaction chamber, the redox potential of the melt would be increased significantly, giving rise to the enhanced dissolution of Ni, Fe and Cr. In a study of the effect of moisture on corrosion of Ni-based alloys in molten (Li,Na,K)F, Ouyang et al. [10] observed that the alloys in molten (Li,Na,K)F with higher moisture content would aggravate intergranular corrosion and pitting. Based on the Nernst Equations and the thermodynamic data from HSC Chemistry version 6.0 database [20], the stability domains of Ni, Fe and Cr as a function of potential and oxoacidity has been established, as shown in Fig. 13 where the red symbols represent the influence of 2% H_2O . Fig. 13 shows clearly that Ni, Fe and Cr are dissolved as Ni^{2+} , $\text{Fe}^{2+}/\text{Fe}^{3+}$, and $\text{Cr}^{2+}/\text{Cr}^{3+}$ in molten (Li,Na,K)F in the presence of

H_2O , respectively. Of the three pure metals, Cr is the most susceptible to dissolution in molten (Li,Na,K)F, with Cr^{3+} as the primary valence state in (Li,Na,K)F [12].

Unlike H_2O , CrF_3 as an oxidizing species could not make the melt be more aggressive to Ni. According to the thermodynamic data from HSC Chemistry version 6.0 database [20], the standard potential $E^\circ(\text{Me}/\text{Me}^{n+})_{\text{vs.}(\text{HF}/\text{H}_2)}$ for the dissolution of Ni, Fe and Cr into molten (Li,Na,K)F at 700 °C has been calculated, as listed in Table 6. Table 6 suggests that Cr^{3+} is a very effective oxidizer to accelerate the dissolution of Cr to form Cr^{2+} , and can also oxidize Fe to form Fe^{2+} to a certain extent, as observed in the present study. However, Cr^{3+} cannot cause the electrochemical dissolution of Ni to form Ni^{2+} . Based on the above polarization and impedance results, it is concluded that the electrochemical cathodic process for the corrosion of Ni in molten (Li,Na,K)F- CrF_3 is mainly related to the reduction of the impurity of H_2O (HF), while that for Cr and Fe mainly involves the reduction of CrF_3 . The corrosion of Cr and Cr-containing alloys in molten fluorides occurs mainly through the dissolution of Cr which

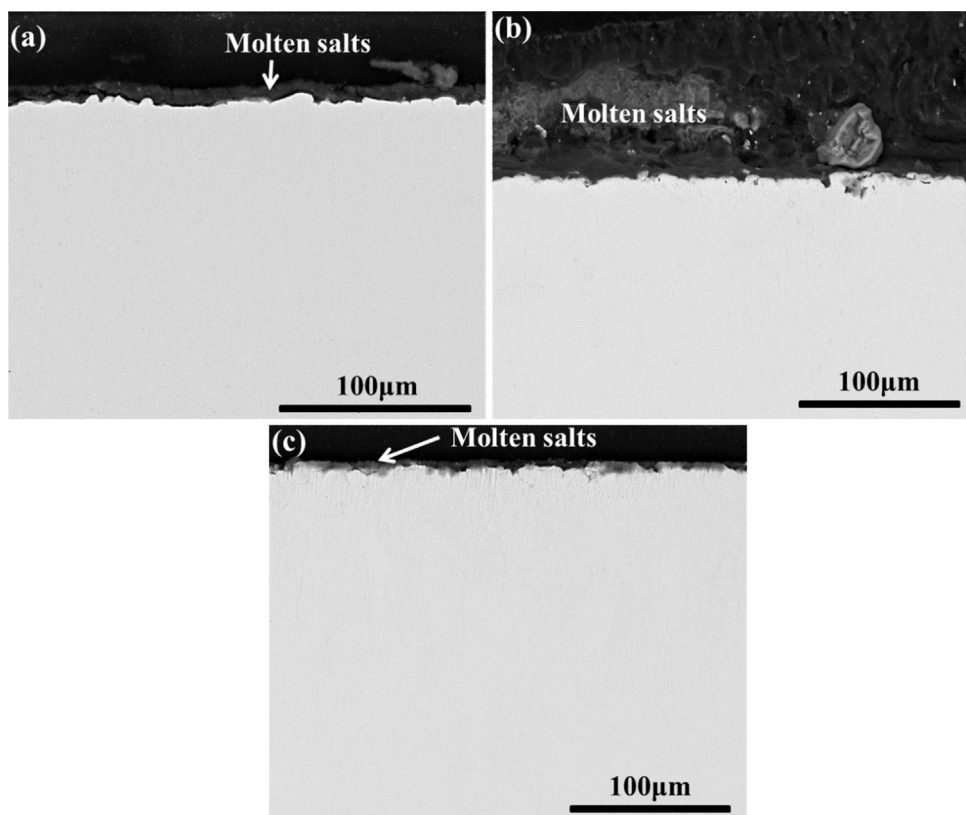


Fig. 10. Cross-sectional morphologies of Ni after immersion in molten $(\text{Li},\text{Na},\text{K})\text{F}$ with 0 M (a), 0.09 M (b) and 0.18 M (c) CrF_3 at 700 °C for 50 h.

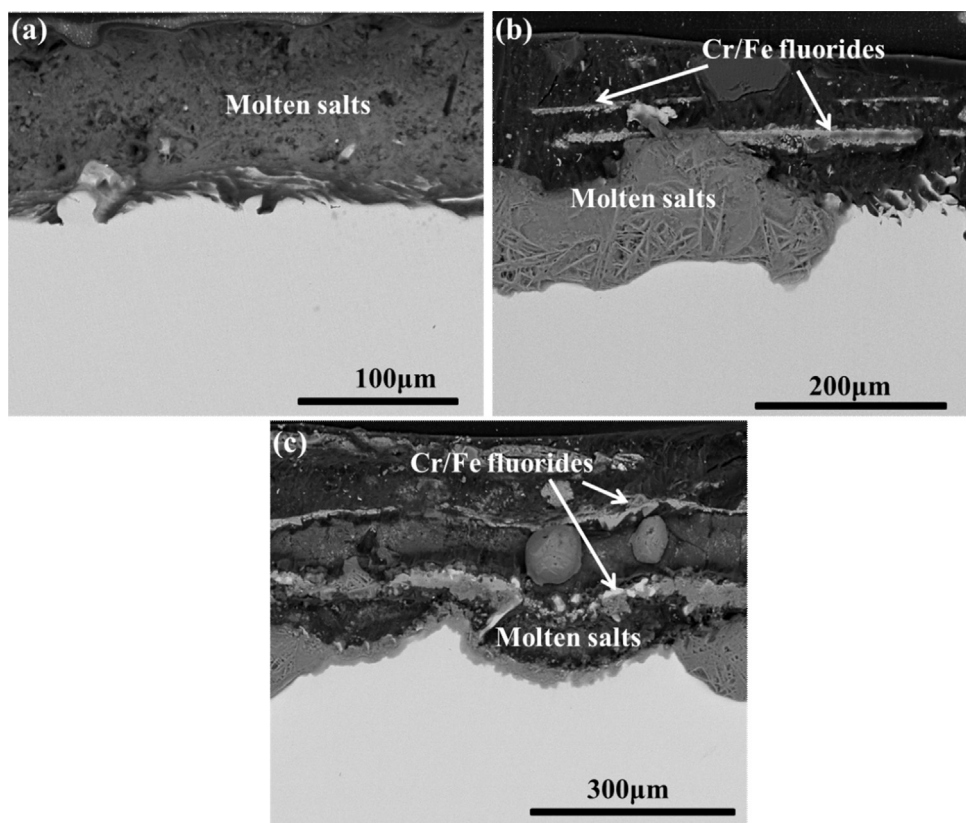


Fig. 11. Cross-sectional morphology of Fe after immersion in molten $(\text{Li},\text{Na},\text{K})\text{F}$ with 0 M (a), 0.09 M (b) and 0.18 M (c) CrF_3 at 700 °C for 50 h.

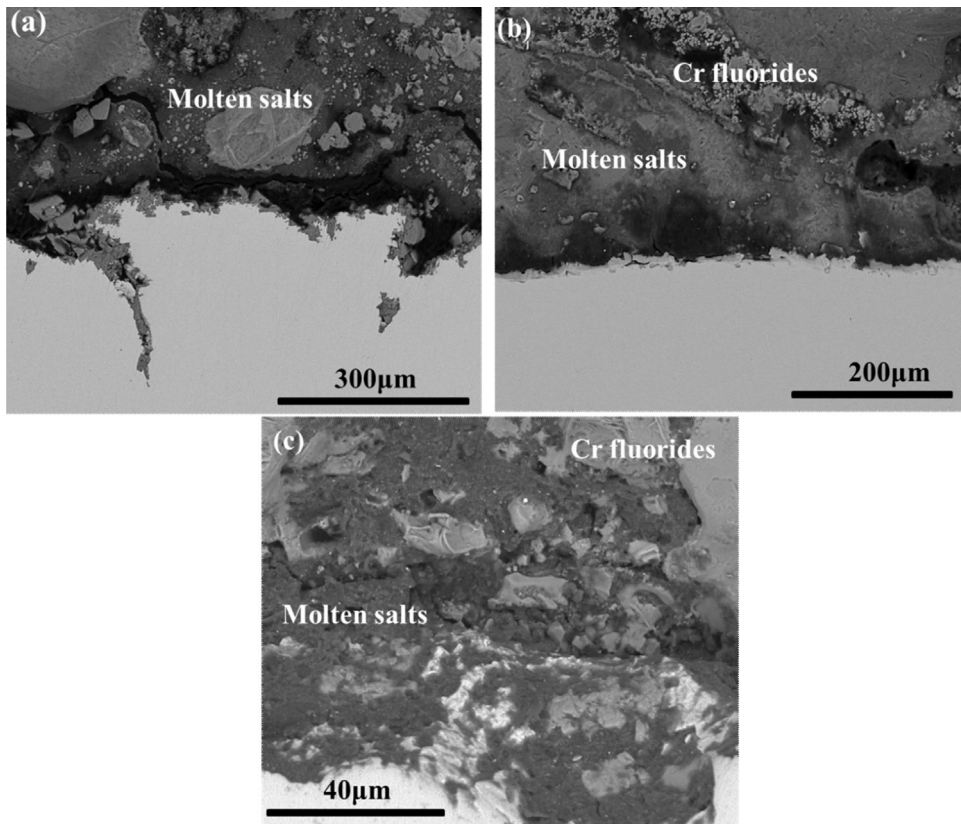


Fig. 12. Cross-sectional morphologies of Cr after immersion in molten (Li,Na,K)F with 0 M (a) CrF₃ for 18 h, 0.09 M (b) and 0.18 M (c) CrF₃ for 13 h at 700 °C.

Table 6

Standard potential $E^\circ_{(\text{Me}/\text{Me}^{n+})\text{vs.}(\text{HF}/\text{H}_2)}$ for the dissolution of Ni, Fe and Cr into molten (Li,Na,K)F at 700 °C [20].

Metals	Reactions	$\Delta G^\circ_{(\text{Me}/\text{Mey}^+)}(\text{kJ mol}^{-1})$	$E^\circ_{(\text{Me}/\text{Mey}^+)\text{vs.}(\text{HF}/\text{H}_2)}(\text{V})$
Ni	$\text{Ni} + 2\text{HF(l)} = \text{NiF}_2 + \text{H}_2(\text{g})$	-64.334	-0.333
Fe	$\text{Fe} + 2\text{HF(l)} = \text{FeF}_2 + \text{H}_2(\text{g})$	-131.981	-0.684
Cr	$\text{Cr} + 2\text{HF(l)} = \text{CrF}_2 + \text{H}_2(\text{g})$	-211.982	-1.098
Cr^{2+}	$\text{CrF}_2 + \text{HF(l)} = \text{CrF}_3 + 0.5\text{H}_2(\text{g})$	-65.123	-0.675

can be promoted by the presence of substantial concentrations of Cr³⁺ in the melt. In the present environments, the corrosion of Cr is determined by the diffusion of Cr³⁺ in the melt. According to the theory of AC impedance for an electrode, the Warburg coefficient, A_w , under the conditions of semi-infinite diffusion is given by Eq. (10) [21,22]:

$$A_w = \sum \frac{RT}{n_i^2 F^2} \left(\frac{1}{C_i \sqrt{D_i}} \right) \quad (10)$$

where i denotes the diffusion species, n_i the electron number for per molecule of species i reduced, F the Faraday constant, and C_i and D_i the solubility and the diffusion coefficient of species i . In molten (Li,Na,K)F-CrF₃, the diffusion species involved in reduction reaction are HF and Cr³⁺. Therefore, Eq. (10) can be expressed as

$$A_w = \frac{RT}{n_{\text{HF}}^2 F^2} \left(\frac{RT}{C_{\text{HF}} \sqrt{D_{\text{HF}}}} \right) + \frac{RT}{n_{\text{Cr}^{3+}}^2 F^2} \left(\frac{1}{C_{\text{Cr}^{3+}} \sqrt{D_{\text{Cr}^{3+}}}} \right) \quad (11)$$

For simplification, the contribution of HF with respect to Cr³⁺ to A_w is neglected, due to the consideration that the corrosion cur-

rent of Cr in the presence of CrF₃ is significantly larger than that in absence of CrF₃. Thus, Eq. (11) can be simplified to

$$A_w = \frac{RT}{n_{\text{Cr}^{3+}}^2 F^2} \left(\frac{1}{C_{\text{Cr}^{3+}} \sqrt{D_{\text{Cr}^{3+}}}} \right) \quad (12)$$

Introducing the value of $A_w = 0.386 \Omega \text{cm}^2 \text{s}^{-0.5}$ for Cr corroded in the melt containing 0.09 M CrF₃ for 18 h, and other parameters into Eq. (12), then the diffusion coefficient of Cr³⁺($D_{\text{Cr}^{3+}}$) is calculated to be $6.25 \times 10^{-4} \text{ cm}^2 \text{s}^{-1}$, which is larger than the value of $5.9 \times 10^{-7} \text{ cm}^2 \text{s}^{-1}$ at 716 °C reported by Yoko and Bailey [23]. CrF₃ could oxidize Cr and Fe by the following reactions:



During the corrosion, a countercurrent diffusion of Cr²⁺/Cr³⁺ could be expected to exist in the melt, and the corrosion reactions could involve these species.

5. Conclusions

Metals Ni, Fe and Cr are all in active dissolution state in molten fluorides at 700 °C at the corrosion potential in Ar environment.

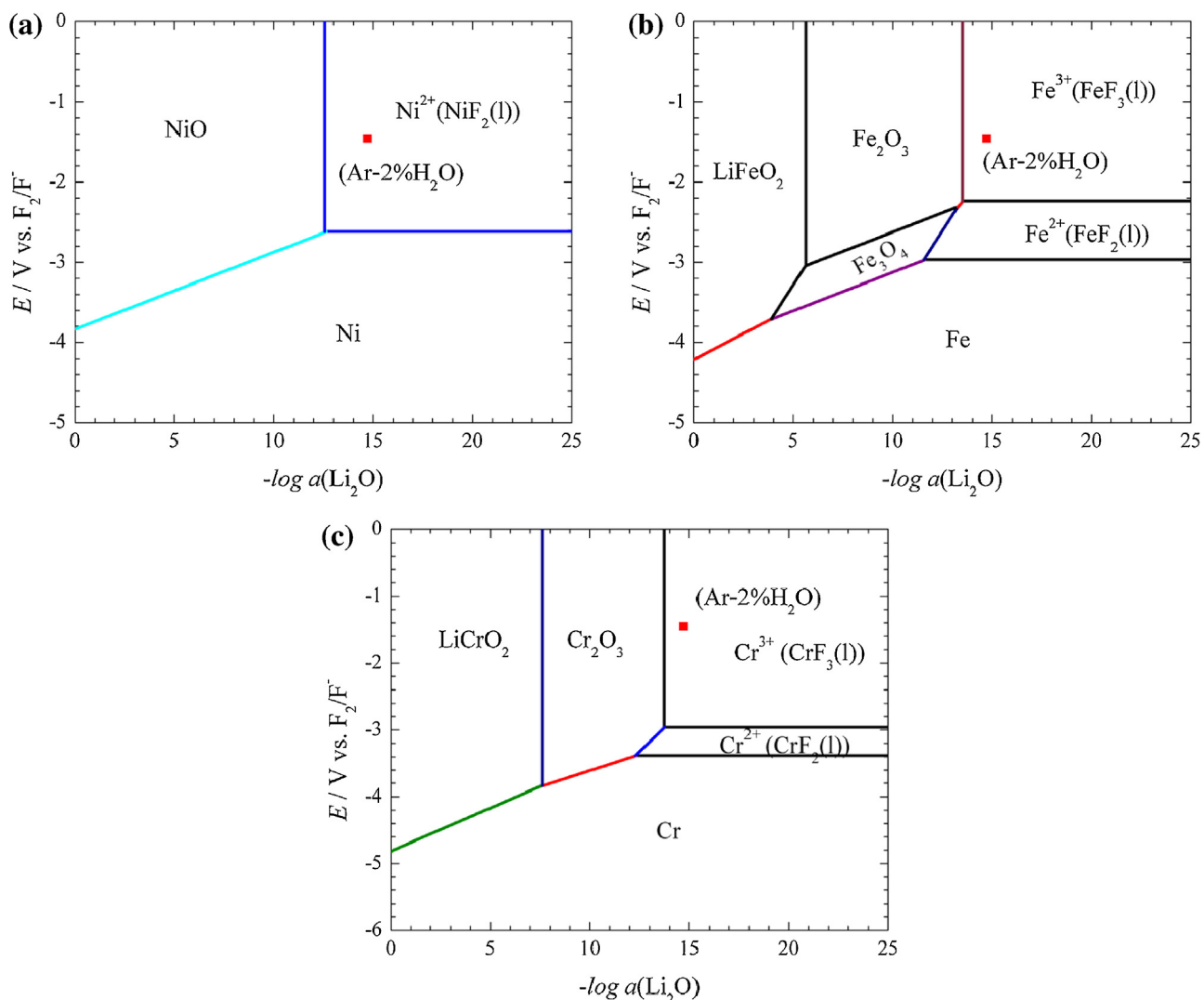


Fig. 13. Potential-oxoacidity diagrams calculated for metals Ni (a), Fe (b) and Cr (c) in molten $(\text{Li}, \text{Na}, \text{K})\text{F}$ ($a(\text{LiF})=0.465$) salt at 700°C [20].

When 2% H_2O is introduced to the environment, Ni, Fe, and Cr are corroded more seriously, with the corrosion rates more than four times higher than those in the absence of 2% H_2O . Differing from H_2O , CrF_3 as an oxidizer can only accelerate the dissolution of Cr and Fe due to the reactions of $2\text{CrF}_3 + \text{Cr} = 3\text{CrF}_2$ and $3\text{CrF}_3 + 1.5 \text{Fe} = 3\text{CrF}_2 + 1.5\text{FeF}_2$, respectively, with a more significant effectiveness for a higher concentration of CrF_3 in the melt. The corrosion of Ni cannot be promoted by CrF_3 , as also confirmed by electrochemical potential calculations. The corrosion of Cr in molten $(\text{Li}, \text{Na}, \text{K})\text{F}-\text{CrF}_3$ is controlled by the diffusion of CrF_3 . Based on the impedance measurements, the diffusion coefficient of Cr^{3+} has been calculated to be $6.25 \times 10^{-4} \text{ cm}^2 \text{ s}^{-1}$. Ni, Fe and Cr all suffer from non-uniform dissolution. Some Cr and Fe enriched fluorides are detected in the melt near the Fe/melt surface. In addition, the dissolution of Cr and Fe in molten $(\text{Li}, \text{Na}, \text{K})\text{F}-\text{CrF}_3$ could involve the species $\text{Cr}^{2+}/\text{Cr}^{3+}$.

Acknowledgement

This work is supported by National Natural Science Foundation of China, Grant No. 51271190 and 51501205.

References

- [1] D.F. Williams, Assessment of candidate molten salt coolant for the NGNP/NHI heat-transfer loop, ORNL/TM-2006/69 (2006).
- [2] H. Zhu, R. Holmes, T. Hanley, J. Davis, K. Short, L. Edwards, High-temperature corrosion of helium ion-irradiated Ni-based alloy in fluoride molten salt, *Corros. Sci.* 91 (2015) 1–6.
- [3] A. Pfennig, B. Fedelich, Oxidation of single crystal PWA 1483 at 950°C in flowing air, *Corros. Sci.* 50 (2008) 2484–2492.
- [4] M. Hofmeister, L. Klein, H. Miran, R. Rettig, S. Virtanen, R.F. Singer, Corrosion behaviour of stainless steels and a single crystal superalloy in a ternary $\text{LiCl}-\text{KCl}-\text{CsCl}$ molten salt, *Corros. Sci.* 90 (2015) 46–53.
- [5] S.M. Jiang, H.Q. Li, J. Ma, C.Z. Xu, J. Gong, C. Sun, High temperature corrosion behaviour of a gradient NiCoCrAlYSi coating II: oxidation and hot corrosion, *Corros. Sci.* 52 (2010) 2316–2322.
- [6] L.C. Olson, J.W. Ambrosek, K. Sridharan, M.H. Anderson, T.R. Allen, Materials corrosion in molten $\text{LiF}-\text{NaF}-\text{KF}$ salt, *J. Fluorine Chem.* 130 (2009) 67–73.
- [7] D. Williams, L. Toth, K. Clarno, Assessment of candidate molten salt coolants for the advanced high temperature reactor (AHTR) ORNL/TM-2006/12 (2006).
- [8] M.W. Rosenthal, P.N. Haubenreich, R.B. Briggs, The development status of molten salt breeder reactors ORNL-4812 (1972).
- [9] M. Sohal, M. Ebner, P. Sabharwall, P. Sharpe, Engineering database of liquid salt thermophysical and thermochemical properties INL/EXT-10-18297 (2010).
- [10] F.Y. Ouyang, C.H. Chang, B.C. You, T.K. Yeh, J.J. Kai, Effect of moisture on corrosion of Ni-based alloys in molten alkali fluoride $\text{LiF}-\text{NaF}$ salt environments, *J. Nucl. Mater.* 437 (2013) 201–207.
- [11] M. Kondo, T. Nagasaka, V. Tsivar, A. Sagara, T. Muroga, T. Watanabe, T. Oshima, Y. Yokoyama, H. Miyamoto, E. Nakamura, N. Fujii, Corrosion of reduced

- activation ferritic martensitic steel JLF-1 in purified Flinak at static and flowing conditions, *Fusion Eng. Des.* 85 (2010) 1430–1436.
- [12] D. Williams, L. Toth, K. Clarno, Assessment of candidate molten salt coolants for the advanced high temperature reactor (AHTR) ORNL/TM2006/12 (2006).
- [13] Y. Wang, H. Liu, C. Zeng, Galvanic corrosion of pure metals in molten fluorides, *J. Fluorine Chem.* 165 (2014) 1–6.
- [14] P. Soucek, F. Lisy, R. Tulackova, J. Uhliar, R. Mraz, Development of electrochemical separation methods in molten LiF-NaF-KF for the molten salt react fuel cycle, *J. Nucl. Sci. Technol.* 42 (2005) 1017–1024.
- [15] J.R. Keiser, J.H. Devan, D.L. Manning, The Corrosion resistance of type 316 stainless steel to Li_2BeF_4 ORNL/TM-5782 (1977).
- [16] A. Conde, J.J. Damborenea, Electrochemical impedance spectroscopy for studying the degradation of enamel coatings, *Corros. Sci.* 44 (2002) 1555–1567.
- [17] M. Lebrini, M. Lagrenée, H. Vezin, M. Traisnel, F. Bentiss, Experimental and theoretical study for corrosion inhibition of mild steel in normal hydrochloric acid solution by some new macrocyclic polyether compounds, *Corros. Sci.* 49 (2007) 2254–2269.
- [18] E. Zahraei, A.M. Alfantazi, Molten salt induced corrosion of Inconel 625 superalloy in $\text{PbSO}_4\text{-Pb}_3\text{O}_4\text{-PbCl}_2\text{-Fe}_2\text{O}_3\text{-ZnO}$ environment, *Corros. Sci.* 65 (2012) 340–359.
- [19] V.V. Ignat'ev, A.I. Surenkov, I.P. Gnidoi, V.I. Fedulov, V.S. Uglov, A.V. Panov, V.S. Sagardze, V.G. Subbotin, A.D. Toropov, V.K. Afonichkin, A.L. Bove, Investigation of the corrosion resistance of nickel-based alloys in fluoride melts, *Atom. Energy* 101 (2006) 730–738.
- [20] HSC Chemistry is a commercial software including a thermochemical database, developed and sold by Outokumpu, Finland. See <http://www.outokumpu.com/hsc> for more details.
- [21] G.M. Schmid, Interfacial impedance and roughness of solid electrodes; gold in perchloric acid, *Electrochim. Acta* 15 (1970) 65–71.
- [22] C.L. Zeng, W. Wang, W.T. Wu, Electrochemical impedance models for molten salt corrosion, *Corros. Sci.* 43 (2001) 787–801.
- [23] T. Yoko, R.A. Bailey, Electrochemical studies of chromium in molten LiF-NaF-KF (FLINAK), *J. Electrochem. Soc.* 131 (1984) 2590–2595.